JOC The Journal of Organic Chemistry

Article

pubs.acs.org/joc

Synthesis of Benziporphyrins and Heterobenziporphyrins and an Assessment of the Diatropic Characteristics of the Protonated Species

Timothy D. Lash,* Ashley M. Toney, Kylie M. Castans, and Gregory M. Ferrence

Department of Chemistry, Illinois State University, Normal, Illinois 61790-4160, United States

Supporting Information

ABSTRACT: Benzitripyrranes were prepared by reacting diphenyl-substituted benzenedicarbinols with excess pyrrole in the presence of $BF_3{\cdot}Et_2O$. These dipyrrolic compounds underwent acid-catalyzed condensations with a pyrrole dialdehyde to afford good yields of diphenylbenziporphyrins, and further reaction with palladium(II) acetate gave stable organometallic derivatives. The X-ray crystal structure of a palladium(II) benziporphyrin showed that the system deviates significantly from planarity. Although the benzitripyrranes failed to give stable macrocyclic products with furan or thiophene dialdehydes, they afforded tetraphenyl heterobenziporphyrins upon reaction with diphenyl-substituted furan- or thiophenedicarbinols and $BF_3{\cdot}Et_2O$. Benziporphyrins and their heteroanalogues showed no indication of a diamagnetic ring current by proton NMR spectroscopy, but addition of TFA gave rise to the formation of weakly diatropic dications.

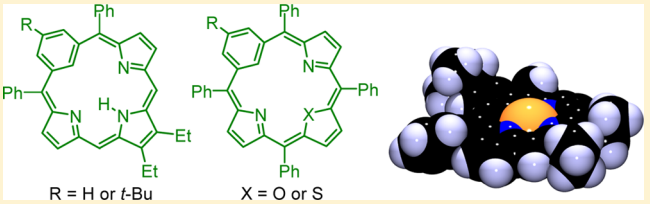

INTRODUCTION

Benziporphyrins (e.g., **1a**) are a family of porphyrin analogues in which one of the pyrrole units has been replaced by a benzene ring.[1,2] This carbaporphyrinoid system was originally prepared by the acid-catalyzed reaction of isophthalaldehyde with a tripyrrane **2** (Scheme 1) followed by oxidation with an electron-deficient quinone (chloranil or DDQ).[1,3,4] An alternative route to *meso*-tetraarylbenziporphyrins **3** was subsequently developed wherein a dicarbinol **4** is reacted with pyrrole and benzaldehyde in the presence of boron trifluoride etherate, followed by oxidation with DDQ (Scheme 2).[5] Diverse benziporphyrin structures have been prepared by both synthetic approaches,[1,4−9] including dimethoxybenziporphyrins **1b**, **1c**, **3c**, and **3d**[6,7] and *tert*-butyl-substituted benziporphyrins **3b**.[8] Benziporphyrins such as **1a** do not exhibit macrocyclic ring currents as determined by proton NMR spectroscopy because of the presence of the cross-conjugated benzene ring,[1,4] but the introduction of electron-donating methoxy groups gives rise to a degree of diatropic character.[6,7] When a hydroxy group is introduced at the 2-position, a tautomerization occurs to give the fully aromatic oxybenziporphyrin system **5** (Scheme 1).[1,4] In this case, the macrocyclic ring current leads to a resonance for the internal CH near −7 ppm. Further oxidized aromatic benziporphyrin

Scheme 1

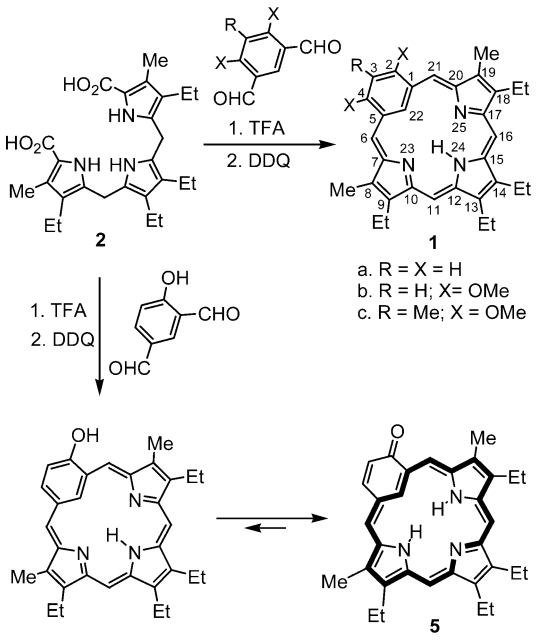

Scheme 2

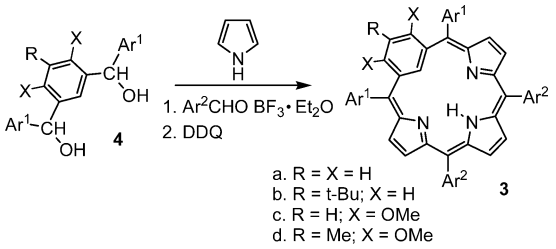

Received: June 22, 2013
Published: August 14, 2013

dx.doi.org/10.1021/jo401365p | J. Org. Chem. 2013, 78, 9143−9152

systems have also been described.[6,10] The coordination chemistry of benziporphyrins has been investigated in detail, and stable organometallic derivatives have also been isolated.[5,7,8,10−12] Furthermore, a dihydrobenziporphyrin has shown promise as a fluorescent zinc cation detector.[13] The metalation of related phthalocyanine analogues has also been investigated.[15]

Addition of TFA to benziporphyrin **1a** affords the corresponding dication $\mathbf{1a}H_2^{2+}$ (Scheme 3).[1] Even though **1a**

Scheme 3

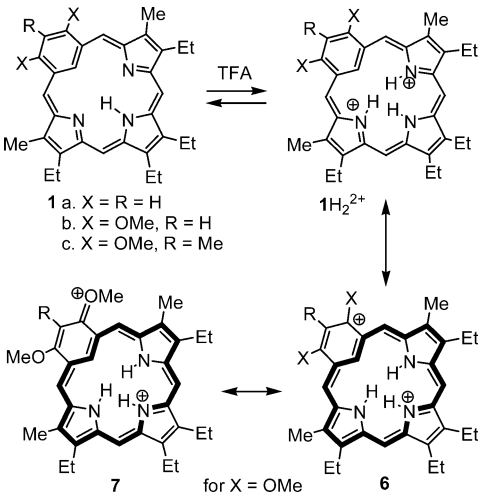

showed no indication of a macrocyclic ring current, the proton NMR spectrum of **1a** in TFA/$CDCl_3$ showed that the internal CH resonance was shifted upfield to 5 ppm.[1,14] This effect was greatly magnified for dimethoxybenziporphyrin dication $\mathbf{1b}H_2^{2+}$, for which the CH resonance was shifted further upfield to −0.68 ppm.[6] The 3-methyl-2,4-dimethoxybenziporphyrin dication $\mathbf{1c}H_2^{2+}$ exhibited an intermediate effect, with the resonance for the internal CH unit showing up at +0.69 ppm.[6] The presence of a macrocyclic ring current in $\mathbf{1a}H_2^{2+}$ was attributed to a resonance contributor **6a** that possesses an 18-π-electron delocalization pathway.[6] Resonance contributors for $\mathbf{1b}H_2^{2+}$ with this type of delocalization pathway are further stabilized by the presence of the methoxy units, which can give rise to canonical forms such as **7b**. However, this type of interaction is less favorable for **1c** because of the presence of a methyl substituent between the two methoxy groups, as the resonance interaction relies upon the OMe groups lying coplanar with the benzene ring, which is inhibited as a result of steric crowding.[6] Similar observations have been made for tetraarylbenziporphyrins **3**.[7,8] These explanations rely upon the diaza[18]annulene model for porphyrinoid aromaticity,[16,17] but this viewpoint has been brought into question.[18,19] Specifically, theoretical studies have indicated that the aromatic character of porphyrins is primarily due to the six-π-electron subunits rather than the presence of 18-π-electron pathways.[18,19] Nevertheless, the diaza[18]annulene model still provides a superior explanation for the aromatic characteristics of many porphyrinoid systems.[17,20] We noted that no examples of heterobenziporphyrins had been prepared previously, although heteroanalogues of many other carbaporphyrinoid systems are known,[21−25] and we speculated that similar borderline aromatic properties might be observed for these systems as well. In view of the high level of interest in benziporphyrin chemistry, these types of heteroporphyrinoids were considered to be worthwhile targets for investigation. In addition, these porphyrinoids might also provide experimental support for the 18-π-electron model for aromaticity in borderline aromatic systems.[17] In this paper, we report the first syntheses of oxa- and thiabenziporphyrins and the preparation of novel *meso*-diphenyl-substituted benziporphyrins.[26]

RESULTS AND DISCUSSION

The synthesis of heterobenziporphyrins was attempted using the "3 + 1" variant of the MacDonald condensation (Scheme 4). In order to carry out these syntheses, benzitripyrranes **8**

Scheme 4

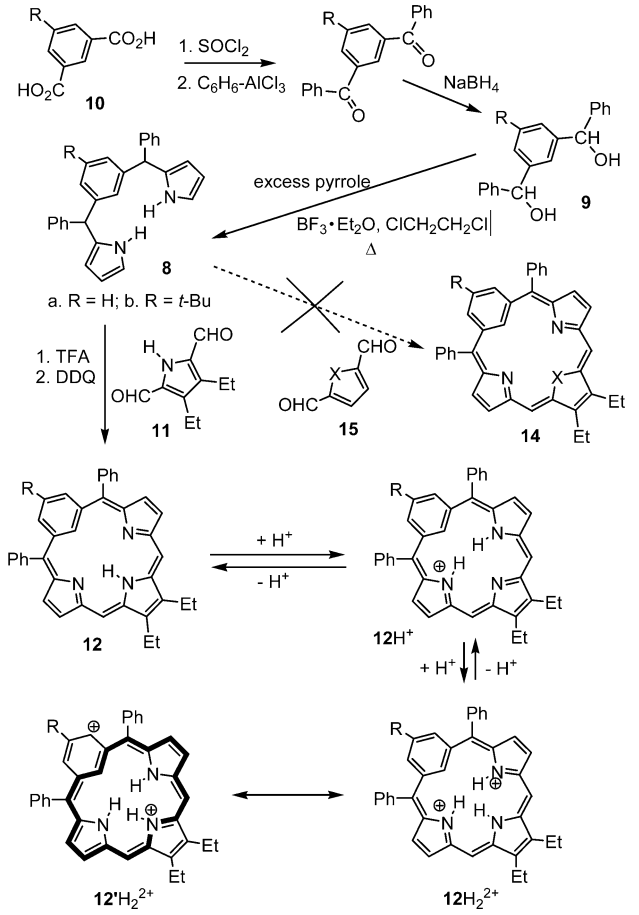

were required as key intermediates. Structures of this type have previously been used in the preparation of porphyrin analogues such as pyriporphyrins[27] and *p*-benziporphyrins.[28] Benzenedicarbinols **9** are easily prepared in multigram quantities from isophthalic acids **10**.[10] Reaction of **9** with excess pyrrole and catalytic boron trifluoride etherate in refluxing 1,2-dichloroethane afforded the required benzitripyrranes **8**. Following column chromatography on silica gel, intermediates **8** were isolated with approximately 95% purity in 66−70% yield. In order to assess the utility of these intermediates, **8a** was reacted with pyrroledialdehyde **11** in the presence of TFA in dichloromethane. After 2 h, DDQ was added to oxidize the initially formed dihydroporphyrinoid, and following extraction and purification by column chromatography on grade-3 alumina, benziporphyrin **12a** was isolated in 50% yield. Dialdehyde **11** similarly reacted with **8b** to give the *tert*-butyl-

dx.doi.org/10.1021/jo401365p | J. Org. Chem. 2013, 78, 9143−9152

substituted benziporphyrin **12b** in 58% yield. The benziporphyrins eluted from the columns in pure form, but recrystallization was not possible because of the highly soluble nature of these porphyrinoids in a wide range of organic solvents, including hexane and methanol.

Benziporphyrins **12** have a unique substitution pattern and may be considered to be hybrids between etio-type benziporphyrins **1** and *meso*-tetrasubstituted benziporphyrins **3**. The UV−vis spectrum of **12b** exhibited a Soret-like band at 403 nm and a broad absorption centered at 656 nm (Figure 1).

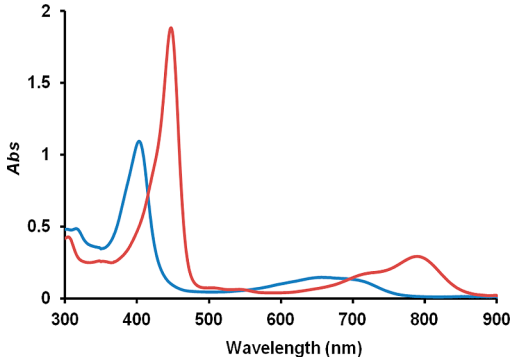

Figure 1. UV−vis spectra of **12b** in 1% Et_3N/CH_2Cl_2 (free base, blue line) and 1% TFA/CH_2Cl_2 (dication $\mathbf{12b}H_2^{2+}$, red line).

In 1% TFA/CH_2Cl_2, a dicationic species $\mathbf{12b}H_2^{2+}$ (Scheme 4) was generated that gave a strong absorption at 447 nm ($\varepsilon > 10^5$ M^{-1} cm^{-1}) and a broad band at 789 nm (Figure 1). Spectrophotometric titration showed the emergence of a peak at 880 nm with 1 equiv of TFA that was attributed to the monoprotonated structure $\mathbf{12b}H^+$, but this species appeared to be in equilibrium with $\mathbf{12b}H_2^{2+}$. Similar results were obtained for benziporphyrin **12a**.

The proton NMR spectra of **12a** and **12b** showed no indication of a macrocyclic ring current. For instance, the proton NMR spectrum of **12b** in $CDCl_3$ showed the outer benzene protons (2,4-H) at 7.04 ppm, while the internal CH appeared at 7.15 ppm (Figure 2). Furthermore, the bridging methine protons (11,16-H) were located at 6.32 ppm, a value that falls into the olefinic region. In the presence of TFA, however, the corresponding dication $\mathbf{12b}H_2^{2+}$ again showed the presence of a recognizable diatropic ring current, as the internal CH shifted upfield to 5.05 ppm, while the external *meso*-protons (11,16-H) moved downfield to 7.03 ppm (Figure 2). The pyrrolic protons of $\mathbf{12b}H_2^{2+}$ gave rise to two doublets of doublets at 7.51 and 7.91 ppm, compared with values of 6.96 and 7.31 ppm for these resonances in the spectrum of the free base. Although the presence of a 2+ charge on the system contributes to the downfield shifts, the data are consistent with the emergence of weak diatropic character over the macrocycle as had been noted for related structures.[1,6,8,14] The dication derived from **12a** in $TFA/CDCl_3$ showed a smaller ring-current effect, as the proton NMR spectrum exhibited a resonance for 22-H at 5.65 ppm while the *meso*-protons (11,16-H) gave rise to a 2H singlet at 6.91 ppm. It has been suggested that the electron-donating *tert*-butyl group helps to stabilize resonance contributors such as **7** that favor the 18-π-electron delocalization pathway.[8]

Benziporphyrins **12a** and **12b** were also characterized by ^{13}C NMR spectroscopy and mass spectrometry. The ^{13}C NMR spectra of **12a** and **12b** confirmed the presence of a plane of symmetry in these macrocycles. The spectrum of **12b** in $CDCl_3$ gave a resonance for the *meso*-CH bridges (11,16-C) at 95.9 ppm, while the internal carbon (22-C) was identified at 109.4 ppm. In $TFA/CDCl_3$, the related dication $\mathbf{12b}H_2^{2+}$ gave a similar value for the *meso*-C resonance at 96.2 ppm, but the 22-C signal was shifted upfield to 96.8 ppm. This compares to

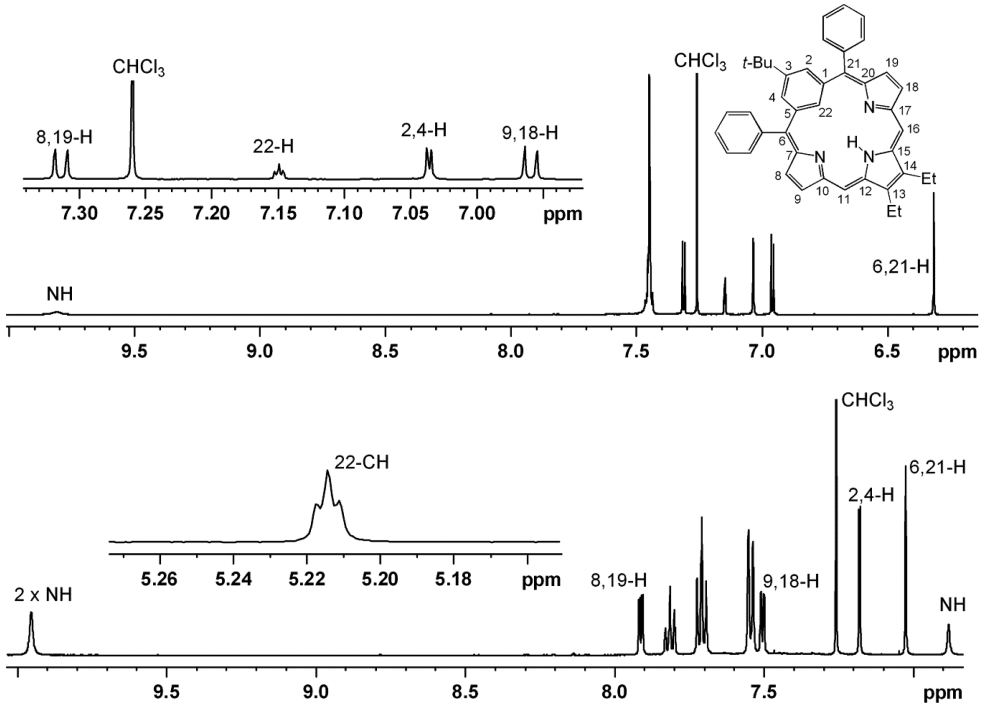

Figure 2. Proton NMR spectra (500 MHz) of *tert*-butyl-substituted benziporphyrin **12b** in $CDCl_3$ (free base, upper spectrum) and $TFA/CDCl_3$ (dication $\mathbf{12b}H_2^{2+}$, lower spectrum).

dx.doi.org/10.1021/jo401365p | J. Org. Chem. 2013, 78, 9143−9152

values of 96.3 and 99.7 ppm, respectively, for dication $12aH_2^{2+}$ in TFA/$CDCl_3$. Benziporphyrins have previously been reported to give a cluster of peaks in the molecular-ion region for electron impact mass spectrometry,[1,3] and this was also the case for **12a** and **12b**. Interestingly, for **12a** the $[M + 2H]^+$ peak at m/z 531 predominated. However, the electrospray ionization mass spectrum for **12a** gave the expected $[M + H]^+$ signal at m/z 530 as the base peak.

As benziporphyrins have been shown to form organometallic derivatives under mild conditions,[7,8,11,14] the preparation of palladium complexes from porphyrinoids **12** was investigated (Scheme 5). Benziporphyrin **12b** was heated with palladium-

Scheme 5

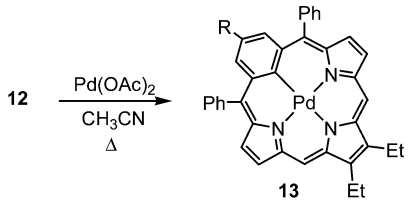

(II) acetate in acetonitrile and gave the corresponding palladium(II) derivative **13b** in 74% yield. Similarly, **12a** reacted with $Pd(OAc)_2$ in refluxing acetonitrile/chloroform to give **13a** in 73% yield. The new organometallic compounds were stable and easily purified by column chromatography on grade-3 basic alumina. The UV–vis spectrum of **13b** gave a Soret-like band at 425 nm (ε = 7.74 × 10^4 M^{-1} cm^{-1}) and a series of minor absorptions between 500 and 850 nm (Figure 3). Although the UV–vis spectrum of **13a** was very similar, the

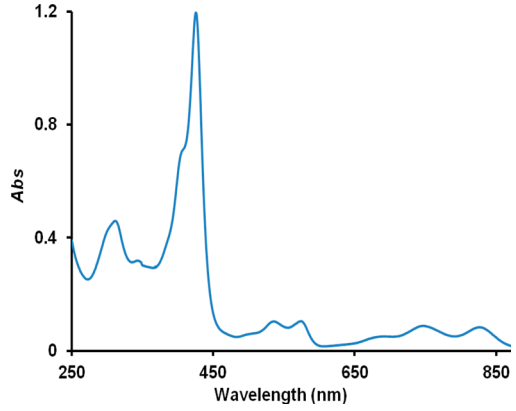

Figure 3. UV–vis spectrum of palladium(II) benziporphyrin **13b** in CH_2Cl_2.

major band underwent a small blue shift to 423 nm. The proton NMR spectrum of **13b** in $CDCl_3$ showed the pyrrolic protons as two 2H doublets at 7.20 and 7.37 ppm, while the *meso*-protons appeared as a 2H singlet at 7.32 ppm. These values are shifted significantly downfield from those noted for the free-base form of **12b**, possibly indicating the presence of a small macrocyclic ring current. The corresponding resonances for **13a** appeared at 7.15, 7.33, and 7.27 ppm, respectively, which are slightly upfield from those of **13b**, again indicating that the *tert*-butyl group enhances the weakly diatropic character of this system. The ^{13}C NMR spectra of **13a** and **13b** demonstrated that the macrocycle had retained a plane of symmetry; **13a** showed the *meso*-CH peak at 99.3 ppm, while **13b** gave this resonance at 99.2 ppm.

The X-ray crystal structure of palladium complex **13b** (Figure 4) both confirms the presence of a benziporphyrin macrocycle

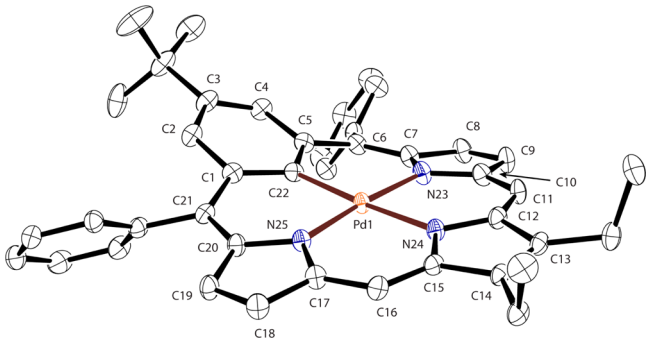

Figure 4. ORTEP-3 drawing (50% probability level, H atoms omitted for clarity) of palladium(II) complex **13b**. Selected bond lengths: C1–C2, 1.414(4); C2–C3, 1.385(4); C3–C4, 1.369(4); C4–C5, 1.418(4); C5–C22, 1.426(4); C22–C1, 1.426(4); C5–C6, 1.451(4); C6–C7, 1.364(4); C7–C8, 1.451(4); C7–N23, 1.391(3); C8–C9, 1.335(4); C9–C10, 1.447(4); C10–N23, 1.356(3); C10–C11, 1.397(4); C11–C12, 1.367(4); C12–N24, 1.369(3); C12–C13, 1.465(3); C13–C14, 1.354(4); C14–C15, 1.464(3); C15–N24, 1.368(3); C15–C16, 1.364(4); C16–C17, 1.391(4); C17–N25, 1.366(3); C17–C18, 1.439(4); C18–C19, 1.3394; C19–C20, 1.450(4); C20–N25, 1.400(3); C20–C21, 1.364(3); C21–C1, 1.453(4).

and demonstrates that the macrocycle deviates significantly from planarity, as evidenced by the rms distance of the framework atoms from the coordination environment plane defined by Pd, C22, N23, N24, and N25 (0.356 Å). Of the 25 framework atoms, 10 deviated from this plane by more than 0.25 Å. The macrocycle is somewhat saddled with the C3-attached *tert*-butyl group at the horn. So defined, the framework arene ring is tilted 19.16(6)° relative to the coordination environment plane with C2 [0.794(3) Å], C3 [0.997(3) Å], and C4 [0.571(3) Å] rising above the plane. The pyrrolic rings adjacent to the framework arene ring are tilted 12.57(9)° and 9.10(8)° relative to the coordination environment plane with C8 [0.538(3) Å], C9 [0.339(3) Å], C18 [0.378(3) Å], and C19 [0.414(3) Å] falling below the plane. The pyrrolic ring opposite to the framework arene ring is tilted 5.73(8)° relative to the coordination environment plane with C13 [0.241(3) Å] and C14 [0.105(3) Å] rising a little above the plane. The larger tilt of the arene ring is attributable to steric repulsion between the C2 and C4 H atoms and the *meso*-phenyl substituents. The phenyl groups are in fact canted 57.61(9)° and 45.61(8)° relative to the coordination environment plane. The structure exhibits framework bond distances consistent with a generally localized π-bonding model. The phenyl substituents attached to the *meso*-carbons have π systems separated from that of the main macrocycle. The metal coordination environment of **13b** is essentially the typical four-coordinate square-planar geometry characteristic of Pd(II) complexes. This is similar to related relatively planar palladium(II) N-confused porphyrins,[29−31] a similar palladium(II) pyrazoloporphyrin,[32] and a closely related palladium(II) naphthiporphyrin.[14] The Pd–C distance of 2.031(2) Å in **13b** is comparable to the distance of 2.055(4) Å observed in a palladium(II) naphthiporphyrin and is consistent with the distances of 2.00(5) Å observed for nearly

dx.doi.org/10.1021/jo401365p | J. Org. Chem. 2013, 78, 9143–9152

3000 crystallographically measured complexes containing Pd–C(phenyl) σ bonds.[33]

Given these successes, it was anticipated that oxa- and thiabenziporphyrins **14** could be synthesized by a similar approach (Scheme 4). However, reaction of furan- or thiophenedialdehyde **15** with benzitripyrranes **8** failed to give more than trace amounts of the benziporphyrin products, although an unstable blue fraction corresponding to a benziphlorin was noted in the furan case. At this stage of the work, an alternative route to oxa- and thiabenziporphyrins was considered. In principle, reactions of **8** with thiophenedicarbinol **16a** and furandicarbinol **16b** could be used to prepare *meso*-tetraphenylheterobenziporphyrins **17** (Scheme 6). Benzitripyrrane **8a** was reacted with **16a** in the presence of boron trifluoride etherate to initially generate benziporphyrinogen **18a**. This species was not isolated but instead was immediately oxidized with DDQ to afford thiabenziporphyrin **17a**. Column chromatography on grade-2 alumina gave a dark-green-colored fraction, and following evaporation of the solvent, **17a** was isolated in 38% yield. The *tert*-butyl-substituted tripyrrane analogue **8b** similarly reacted with **16a** to give thiabenziporphyrin **17b** in 30% yield.

Scheme 6

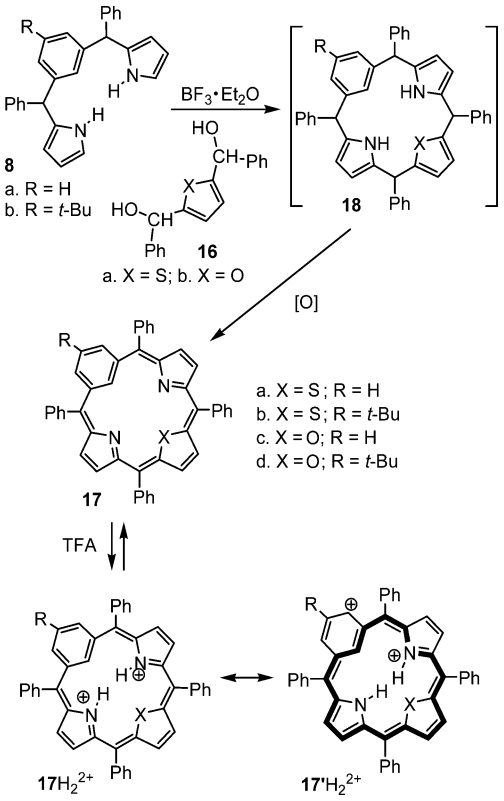

The UV–vis spectrum of **17b** in 1% Et_3N/CH_2Cl_2 gave a moderately strong band at 416 nm and a broad absorption at 643 nm (Figure 5). Porphyrinoid **17a** gave a similar UV–vis spectrum, but the Soret-like band was hypsochromically shifted to 411 nm. Addition of TFA to the solution of **17b** afforded a diprotonated species that showed a strong absorption at 477 nm and broad long-wavelength absorptions at 703 and 880 nm (Figure 5). Again, the UV–vis spectrum of **17a**H_2^{2+} showed a slightly blue-shifted Soret-like band at 475 nm. Addition of 1 equiv of TFA to a solution of **17a** or **17b** in dichloromethane

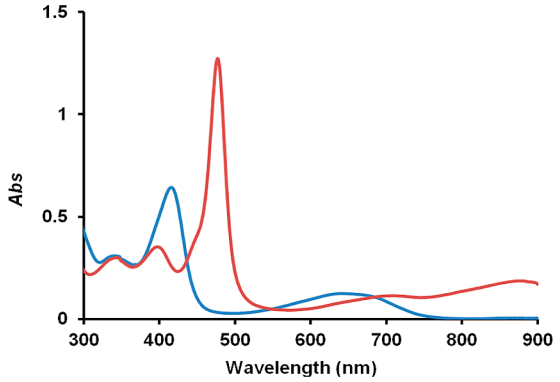

Figure 5. UV–vis spectra of thiabenziporphyrin **17b** in 1% Et_3N/CH_2Cl_2 (free base, blue line) and 1% TFA/CH_2Cl_2 (dication **17b**H_2^{2+}, red line).

resulted in the appearance of a broad peak near 800 nm that was attributed to monocations **17**H^+, but as was the case for benziporphyrins **12a** and **12b**, these appeared to be in equilibrium with the dicationic species **17**H_2^{2+}.

The proton NMR spectra of **17a** and **17b** were consistent with a system that lacks macrocyclic aromatic character. For instance, in the proton NMR spectrum of **17b**, the internal 22-H gave a 1H triplet (J = 1.5 Hz) at 7.04 ppm, while the outer benzene protons (2,4-H) appeared as a 2H doublet at 7.10 ppm. However, in TFA/$CDCl_3$, the resulting dication **17b**H_2^{2+} exhibited a degree of diatropic character (Figure 6), as the internal CH appeared as an upfield triplet (J = 1.5 Hz) at 4.93 ppm while the external benzene hydrogens (2,4-H) gave a 2H doublet further downfield at 7.35 ppm. The pyrrolic protons were also shifted further downfield to give resonances at 7.23 and 7.97 ppm, while the thiophene protons gave a singlet at 8.00 ppm. All of these shifts were slightly reduced for **17a**H_2^{2+} in TFA/$CDCl_3$, and the internal CH showed up at 5.29 ppm in this case. These data indicate that the dications derived from thiabenziporphyrins, like those derived from benziporphyrins,

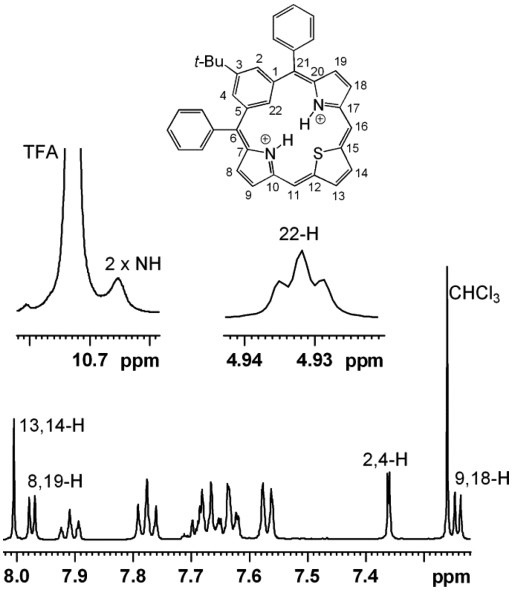

Figure 6. Proton NMR spectrum (500 MHz) of thiabenziporphyrin dication **17b**H_2^{2+} in TFA/$CDCl_3$. The internal CH shows up as a triplet at 4.93 ppm.

dx.doi.org/10.1021/jo401365p | J. Org. Chem. 2013, 78, 9143–9152

possess a significant degree of diatropic character and that the presence of the *tert*-butyl substituent again enhances this effect. Both the proton and ^{13}C NMR spectra of **17a** and **17b** demonstrated the presence of a plane of symmetry in these ring systems. For spectra run in $CDCl_3$, the internal C resonances of **17a** and **17b** appeared at 113.0 and 110.8 ppm, respectively, but in TFA/$CDCl_3$ the peaks for the corresponding dications shifted upfield to values of 100.2 and 98.1 ppm. In this respect, the results resembled those obtained for benziporphyrins **12a** and **12b**. In addition, the electron impact mass spectra of thiabenziporphyrins **17a** and **17b** gave a cluster of peaks in the molecular-ion region, as observed for benziporphyrins **12**.

Benzitripyrranes **8a** and **8b** also reacted with furandicarbinol **16b** to give the related oxabenziporphyrins **17c** and **17d**, respectively (Scheme 6). However, difficulties were encountered in purifying these porphyrinoids. Protonation of the system occurred readily, and the best results were obtained when the structures were deliberately protonated prior to purification. The oxidation was carried out with DDQ in the presence of TFA. The reaction solutions were washed with sodium bicarbonate solution and then with 10% hydrochloric acid, and the solvent was removed on a rotary evaporator. The protonated mixture was run through a silica column, and the products were obtained in a partially protonated form in 28% yield. The isolated porphyrinoids appeared to be primarily in the monoprotonated form. The UV−vis spectrum of **17d** in dichloromethane gave a series of bands at 352, 381, 452, and 806 nm with a stronger absorption at 265 nm, but in 5% Et_3N/CH_2Cl_2 only broad absorptions were noted at 385 and 637 nm (Figure 7). The latter spectrum was attributed to the free-base

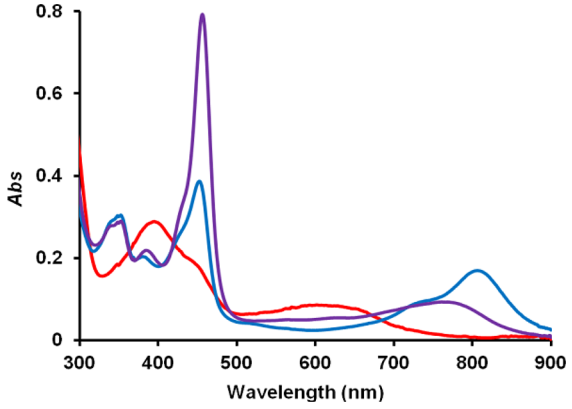

Figure 7. UV−vis spectra of oxabenziporphyrin **17d** in 5% Et_3N/CH_2Cl_2 (free base, red line), CH_2Cl_2 (blue line), and 1% TFA/CH_2Cl_2 (dication **17d**H_2^{2+}, purple line).

form of the macrocycle. In 1% TFA/CH_2Cl_2, **17d**H_2^{2+} gave a completely different spectrum with a strong Soret-like band at 456 nm and weaker absorptions at 352, 384, and 768 nm (Figure 7). Similar results were obtained for oxabenziporphyrin **17c**.

The proton NMR spectra of the diprotonated oxabenziporphyrins were obtained in TFA/$CDCl_3$. The *tert*-butyl-substituted structure **17d** showed the presence of a 1H triplet (J = 1.5 Hz) corresponding to the internal CH at 5.30 ppm. The pyrrolic protons produced two doublets of doublets at 7.00 and 7.83 ppm, while the furan protons appeared as a 2H singlet at 7.50 ppm. Oxabenziporphyrin **17c** showed the internal CH at 5.65 ppm, the pyrrolic protons at 6.98 and 7.81 ppm, and the furan protons at 7.48 ppm. These data indicate that the *tert*-butyl group in **17d** is again responsible for a small increase in the diatropicity. The chemical shifts for tetraphenylbenziporphyrin dications **3**H_2^{2+} in TFA/$CDCl_3$ have been reported previously.[8] In order to compare the diatropic characters of the benziporphyrins and heterobenziporphyrins, only resonances that are not directly affected by the heteroatom substitution were considered. For this discussion, the external pyrrole protons at positions 9,18 and 8,19 were examined, as well as the internal 22-H (Table 1). On the basis of the downfield shifts for

Table 1. Selected Chemical Shifts (ppm) for Benziporphyrin and Heterobenziporphyrin Dications in TFA/$CDCl_3$

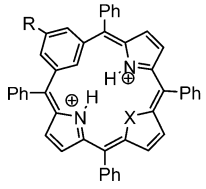

3aH_2^{2+} X = NH; R = H
3bH_2^{2+} X = NH; R = *t*-Bu
17aH_2^{2+} X = S; R = H
17bH_2^{2+} X = S; R = *t*-Bu
17cH_2^{2+} X = O; R = H
17dH_2^{2+} X = O; R = *t*-Bu

	22-H	9,18-H	8,19-H
3aH_2^{2+} [a]	5.65	7.08	7.79
3bH_2^{2+} [a]	5.05	7.12	7.96
17aH_2^{2+}	5.29	7.22	7.97
17bH_2^{2+}	4.93	7.23	7.97
17cH_2^{2+}	5.65	6.98	6.98
17dH_2^{2+}	5.27	7.81	7.81

[a]Data taken from ref 8.

the external pyrrolic protons and the upfield shifts for 22-H, the thiabenziporphyrin dications showed the largest diatropic ring currents while the oxabenziporphyrins showed the smallest effects. For each system, the presence of a *tert*-butyl group significantly increased the diatropicity for the macrocycle. The electronegative oxygen atom in **17c**H_2^{2+} and **17d**H_2^{2+} is less effective in facilitating charge delocalization, which provides an explanation for the reduced shifts observed for these dications. On the other hand, sulfur enhances the aromatic character of thiophene compared with pyrrole or furan and presumably exerts a similar effect for **17a**H_2^{2+} and **17b**H_2^{2+}. The ^{13}C NMR spectra of oxabenziporphyrin dications **17c**H_2^{2+} and **17d**H_2^{2+} in TFA/$CDCl_3$ confirmed that these structures also possess a plane of symmetry and again showed the internal C resonance (22-C) at relatively upfield values of 104.4 and 101.7 ppm, respectively.

CONCLUSION

Tripyrrane analogues have been prepared by reacting benzenedicarbinols with excess pyrrole in the presence of boron trifluoride etherate, and these intermediates were used to prepare diphenylbenziporphyrins by carrying out acid-catalyzed condensations with a pyrroledialdehyde. Protonation with TFA afforded dicationic species that showed significant, albeit relatively small, diamagnetic ring currents. These novel benziporphyrins also smoothly reacted with palladium(II) acetate to give the related organometallic derivatives, and a palladium(II) complex was characterized by X-ray crystallography. Attempts to react benzitripyrranes with furan- or thiophenedialdehyde failed to give macrocyclic products. However, the benzitripyrranes did condense with furan- or thiophenedicarbinols in the presence of boron trifluoride etherate to give the first examples of tetraphenyl-substituted oxa- and thiabenziporphyrins. Diprotonation of heterobenzi-

dx.doi.org/10.1021/jo401365p | J. Org. Chem. 2013, 78, 9143−9152

porphyrins also gave rise to dications with diatropic character. The shifts observed for oxabenziporphyrins were slightly smaller than those observed for structurally similar benziporphyrins, but thiabenziporphyrin dications exhibited enhanced diatropicity. These results give further insights into the aromatic characteristics of porphyrinoid systems and provide access to hitherto-unknown heterobenziporphyrin structures.

EXPERIMENTAL SECTION

Melting points are uncorrected. UV−vis data are reported as λ_{max}/nm ($\log[\varepsilon/M^{-1}\ cm^{-1}]$). NMR spectra were recorded using a 400 or 500 MHz NMR spectrometer. ^{1}H NMR values are reported as chemical shift (δ), relative integral, multiplicity (s, singlet; d, doublet; t, triplet; q, quartet; m, multiplet; br, broad peak), and coupling constant (J). Chemical shifts are reported in parts per million relative to $CDCl_3$ (^{1}H residual $CHCl_3$, δ 7.26; ^{13}C $CDCl_3$ triplet, δ 77.23), and coupling constants were taken directly from the spectra. NMR assignments were made with the aid of ^{1}H−^{1}H COSY, HSQC, DEPT-135, and NOE difference proton NMR spectroscopy. 2D NMR experiments were performed using standard software. High-resolution mass spectrometry (HRMS) was carried out using a double-focusing magnetic sector instrument. ^{1}H and ^{13}C NMR spectra for all of the new compounds are reported in the Supporting Information.

1,3-Bis(phenylpyrrolylmethyl)benzene (8a). Nitrogen was bubbled through a solution of bis(phenylhydroxymethyl)benzene[8] (580 mg, 2.00 mmol) and pyrrole (20 mL) in 1,2-dichloroethane (40 mL) for 20 min, after which 1.5 mL of a 10% $BF_3{\cdot}Et_2O$ solution in dichloromethane was added and the resulting mixture was stirred under reflux for 16 h. The solution was cooled to room temperature, and the reaction was quenched by addition of triethylamine (2 mL). The solvent was removed on a rotary evaporator at aspirator pressures, and then an oil pump was attached to remove excess pyrrole. The product was purified by column chromatography on silica, eluting with a mixture of hexanes, dichloromethane, and triethylamine in a ratio of 60:40:1. Evaporation of the product fractions gave the benzitripyrrane (0.51 g, 1.31 mmol, 66%) as a pale-colored oil that was stored in the freezer. The NMR data were consistent with the presence of two diastereomers. ^{1}H NMR (500 MHz, $CDCl_3$): δ 5.253, 5.256 (2H, two overlapping singlets), 5.65 (2H, m), 6.01 (2H, m), 6.51 (2H, m), 6.92 (2H, dd, J = 1.8, 7.6 Hz), 6.98−7.00 (1H, two overlapping triplets, J = 2.0 Hz), 7.03 (4H, d, J = 7.6 Hz), 7.09−7.13 (3H, m), 7.17 (4H, t, J = 7.6 Hz), 7.56 (2H, br s). ^{13}C NMR ($CDCl_3$): δ 50.68, 50.70, 108.11, 108.13, 108.4, 117.3, 126.8, 127.30, 127.31, 128.6, 128.8, 129.0, 129.79, 129.81, 133.7, 143.2, 143.47, 143.49. HRMS (EI) m/z: calcd for $C_{28}H_{24}N_2$, 388.1939; found, 388.1943.

5-*tert*-Butyl-1,3-bis(phenylpyrrolylmethyl)benzene (8b). Under the same conditions as described above for **8a**, dicarbinol **9b**[8] reacted with pyrrole (20 mL) to give the tripyrrane analogue (0.62 g, 1.4 mmol, 70%) as a pale-colored oil that solidified upon standing in the freezer. The NMR data were consistent with the presence of two diastereomers. ^{1}H NMR (500 MHz, $CDCl_3$): δ 1.13 (9H, s), 5.29 (2H, s), 5.66−5.68 (2H, m), 6.03−6.05 (2H, m), 6.57−6.59 (2H, m), 6.77−6.79 (1H, two overlapping triplets, J = 1.6 Hz), 7.01 (2H, d, J = 1.6 Hz), 7.06 (4H, d, J = 7.7 Hz), 7.11−7.15 (2H, m), 7.17−7.21 (4H, m), 7.64 (2H, br s). ^{13}C NMR ($CDCl_3$): δ 31.5, 34.9, 51.05, 51.07, 108.1, 108.4, 117.2, 124.6, 126.7, 126.8, 128.6, 129.0, 134.03, 134.05, 142.8, 143.53, 143.55, 151.7. HRMS (EI) m/z: calcd for $C_{32}H_{32}N_2$ 444.2565; found 444.2560.

13,14-Diethyl-6,21-diphenylbenziporphyrin (12a). Benzitripyrrane **8a** (85 mg, 0.22 mmol) and pyrroledialdehyde **11**[34] (39.4 mg, 0.22 mmol) were dissolved in dichloromethane (100 mL), and nitrogen was bubbled through the solution for 5 min. TFA (1 mL) was then added, and the resulting solution was stirred in the dark under nitrogen at room temperature for 2 h. DDQ (51 mg) was added, and the mixture was stirred for a further 1 h. The solution was washed with 5% aqueous sodium bicarbonate solution and water, and the solvent was removed under reduced pressure. The residue was purified on a grade-3 alumina column, eluting with dichloromethane, and the product was collected as a dark-green band. Evaporation of the solvent gave the benziporphyrin (56.8 mg, 0.11 mmol, 50%) as a dark-green solid. Mp: >300 °C. UV−vis (1% Et_3N/CH_2Cl_2) λ_{max} (log ε): 314 (4.55), 399 (4.87), 663 (3.99). UV−vis (1% TFA/CH_2Cl_2) λ_{max} (log ε): 303 (4.42), 347 (4.32), 446 (5.14), 712 (sh, 4.06), 786 (4.31). ^{1}H NMR (500 MHz, $CDCl_3$): δ 1.28 (6H, t, J = 7.6 Hz, 2 × CH_2CH_3), 2.70 (4H, q, J = 7.6 Hz, 13,14-CH_2), 6.28 (2H, s, 11,16-H), 6.94 (2H, d, J = 4.7 Hz, 9,18-H), 6.99 (2H, dd, J = 1.8, 7.8 Hz, 2,4-H), 7.24 (2H, t, J = 7.8 Hz, 3-H), 7.28 (2H, d, J = 4.7 Hz, 8,19-H), 7.41−7.48 (11H, m, 22-H + 2 × Ph), 9.99 (1H, br s, NH). ^{1}H NMR (500 MHz, TFA/$CDCl_3$): δ 1.29 (6H, t, J = 7.6 Hz, 2 × CH_2CH_3), 2.84 (4H, q, J = 7.6 Hz, 13,14-CH_2), 5.79 (1H, br t, J = 1.7 Hz, 22-H), 6.91 (2H, s, 11,16-H), 7.14 (2H, dd, J = 1.7, 7.8 Hz, 2,4-H), 7.44 (2H, d, J = 5.0 Hz, 9,18-H), 7.52 (4H, d, J = 7.7 Hz, 4 × o-H), 7.67 (4H, t, J = 7.7 Hz, 4 × m-H), 7.68 (1H, t, J = 7.8 Hz, 3-H), 7.77 (2H, t, J = 7.5 Hz, 2 × p-H), 7.83 (2H, d, J = 5.0 Hz, 8,19-H), 10.52 (2H, br s, 23,25-H). ^{13}C NMR ($CDCl_3$): δ 15.8, 17.9, 96.0, 111.7, 127.2, 128.1, 128.5, 130.9, 132.9, 134.0, 137.8, 138.1, 140.3, 142.6, 143.3, 148.4, 156.7. ^{13}C NMR (TFA/$CDCl_3$): δ 15.1, 18.3, 96.3, 99.7, 128.8, 129.0, 132.8, 132.9, 134.9, 136.3, 138.2, 139.4, 139.6, 143.8, 146.2, 151.1, 153.4, 161.2. HRMS (ESI) m/z: calcd for $C_{38}H_{31}N_3$ + H, 530.2596; found, 530.2293.

3-*tert*-Butyl-13,14-diethyl-6,21-diphenylbenziporphyrin (12b). Tripyrrane analogue **8b** (97.5 mg, 22 mmol) was reacted with **11** (39.4 mg, 0.22 mmol) under the foregoing conditions for **12a** to give benziporphyrin **12b** (74.5 mg, 0.127 mmol, 58%) as a dark solid. Mp: >300 °C. UV−vis (1% Et_3N/CH_2Cl_2) λ_{max} (log ε): 315 (4.48), 403 (4.83), 656 (3.96). UV−vis (1% TFA/CH_2Cl_2) λ_{max} (log ε): 447 (5.07), 789 (4.26). ^{1}H NMR (500 MHz, $CDCl_3$): δ 0.96 (9H, s, t-Bu), 1.28 (6H, t, J = 7.6 Hz, 2 × CH_2CH_3), 2.72 (4H, q, J = 7.6 Hz, 13,14-CH_2), 6.32 (2H, s, 11,16-H), 6.96 (2H, d, J = 4.6 Hz, 9,18-H), 7.04 (2H, d, J = 1.6 Hz, 2,4-H), 7.15 (1H, t, J = 1.6 Hz, 22-H), 7.31 (2H, d, J = 4.6 Hz, 8,19-H), 7.44−7.47 (10H, m, 2 × Ph), 9.81 (1H, br s, NH). ^{1}H NMR (500 MHz, TFA/$CDCl_3$): δ 1.05 (9H, s, t-Bu), 1.31 (6H, t, J = 7.7 Hz, 2 × CH_2CH_3), 2.86 (4H, q, J = 7.7 Hz, 13,14-CH_2), 5.21 (1H, t, J = 1.6 Hz, 22-H), 6.88 (1H, br s, 24-NH), 7.03 (2H, s, 11,16-H), 7.18 (2H, d, J = 1.6 Hz, 2,4-H), 7.51 (2H, dd, J = 1.2, 5.0 Hz, 9,18-H), 7.54 (4H, d, J = 7.7 Hz, 4 × o-H), 7.71 (4H, t, J = 7.7 Hz, 4 × m-H), 7.82 (2H, t, J = 7.5 Hz, 2 × p-H), 7.91 (2H, dd, J = 1.3, 5.0 Hz, 8,19-H), 9.95 (1H, br s, 23,25-NH). ^{13}C NMR ($CDCl_3$): δ 15.9, 17.9, 30.9, 34.6, 95.9, 109.4, 127.1, 128.0, 130.6, 131.6, 133.1, 137.6, 137.8, 140.2, 143.3, 143.4, 148.1, 150.5, 156.6, 170.1. ^{13}C NMR (TFA/$CDCl_3$): δ 15.0, 18.3, 30.4, 35.5, 96.2, 96.8, 128.8, 129.1, 133.4, 134.3, 135.3, 138.1, 139.5, 143.8, 146.3, 152.2, 152.9, 156.9, 160.7. HRMS (EI) m/z: calcd for $C_{42}H_{39}N_3$, 585.3144; found, 585.3138.

(13,14-Diethyl-6,21-diphenylbenziporphyrinato)palladium(II) (13a). Benziporphyrin **12a** (15.0 mg, 0.028 mmol) and palladium(II) acetate (15 mg) in acetonitrile (15 mL) were heated under reflux for 30 min. The solution was cooled to room temperature, diluted with dichloromethane, and washed with water, and the organic solution was evaporated under reduced pressure. The residue was purified by column chromatography on grade-3 basic alumina, eluting with chloroform, and the product was collected as a red-brown fraction. Recrystallization from chloroform/methanol gave the palladium complex (12.9 mg, 0.020 mmol, 73%) as dark crystals. Mp: 269−270 °C. UV−vis (CH_2Cl_2) λ_{max} (log ε): 310 (4.46), 403 (sh, 4.62), 423 (4.87), 499 (sh, 3.50), 535 (3.70), 573 (3.64), 680 (sh, 3.46), 747 (3.75), 825 (3.71). ^{1}H NMR (500 MHz, $CDCl_3$): δ 1.41 (6H, t, J = 7.6 Hz, 2 × CH_2CH_3), 2.95 (4H, q, J = 7.6 Hz, 13,14-CH_2), 7.15 (2H, d, J = 5.0 Hz, 8,19-H), 7.18 (2H, t, J = 7.7 Hz, 3-H), 7.27 (2H, s, 11,16-H), 7.33 (2H, d, J = 5.0 Hz, 9,18-H), 7.44−7.52 (6H, m, m-H + p-H), 7.56−7.59 (4H, m, 4 × o-H), 7.81 (2H, d, J = 7.7 Hz, 2,4-H). ^{13}C NMR ($CDCl_3$): δ 16.5, 18.5, 99.3, 124.8, 126.6, 127.5, 130.7, 132.5, 134.3, 136.3, 142.2, 142.6, 142.8, 143.2, 144.1, 145.2, 153.4, 157.8. HRMS (EI) m/z: calcd for $C_{38}H_{29}N_3Pd$, 633.1396; found, 633.1402.

(3-*tert*-Butyl-13,14-diethyl-6,21-diphenylbenziporphyrinato)palladium(II) (13b). Benziporphyrin **12b** (20 mg, 0.034 mmol) and palladium(II) acetate (20 mg) were reacted in a mixture of chloroform (10 mL) and acetonitrile (10 mL) under the foregoing conditions for **13a**. Recrystallization from chloroform/methanol gave the palladium complex (17.3 mg, 0.025 mmol, 74%) as dark crystals.

dx.doi.org/10.1021/jo401365p | J. Org. Chem. 2013, 78, 9143−9152

Mp: 239−240 °C. UV−vis (CH_2Cl_2) λ_{max} (log ε): 311 (4.47), 405 (sh, 4.66), 425 (4.89), 499 (sh, 3.58), 535 (3.83), 574 (3.83), 689 (sh, 3.51), 747 (3.75), 826 (3.73). ^{1}H NMR (500 MHz, $CDCl_3$): δ 1.01 (9H, s, *t*-Bu), 1.43 (6H, t, J = 7.6 Hz, 2 × CH_2CH_3), 2.98 (4H, q, J = 7.6 Hz, 13,14-CH_2), 7.20 (2H, d, J = 5.0 Hz, 8,19-H), 7.32 (2H, s, 11,16-H), 7.37 (2H, d, J = 5.0 Hz, 9,18-H), 7.45−7.53 (6H, m, *m*-H + *p*-H), 7.59−7.61 (4H, m, 4 × *o*-H), 7.90 (2H, s, 2,4-H). ^{13}C NMR ($CDCl_3$): δ 16.6, 18.5, 30.6, 34.1, 99.2, 126.4, 127.5, 130.5, 132.5, 134.0, 136.2, 140.5, 142.8, 143.1, 144.0, 145.1, 146.1, 153.1, 157.4. HRMS (EI) m/z: calcd for $C_{42}H_{37}N_3Pd$, 689.2022; found, 689.2035.

6,11,16,21-Tetraphenyl-24-thiabenziporphyrin (17a). Nitrogen was bubbled through a solution of thiophenedicarbinol **16a**[35] (85.8 mg, 0.29 mmol) and benzitripyrrane **8a** (112.5 mg, 0.29 mmol) in dichloromethane (90 mL) for 10 min, and 200 μL of a 10% BF_3·Et_2O solution in dichloromethane was then added. The resulting solution was stirred in the dark at room temperature under nitrogen for 2 h. DDQ (194 mg) was added, and the mixture was stirred for a further 30 min. The mixture was washed with water, and the solvent was evaporated under reduced pressure. The residue was chromatographed on a grade-2 alumina column, eluting with dichloromethane, and the product was collected as a bright-green band. Evaporation of the solvent under reduced pressure gave the thiabenziporphyrin (70.5 mg, 0.11 mmol, 38%) as a dark solid. Mp: >300 °C. UV−vis (1% Et_3N/CH_2Cl_2) λ_{max} (log ε): 335 (4.40), 411 (4.70), 643 (4.03). UV−vis (1% TFA/CH_2Cl_2) λ_{max} (log ε): 346 (4.42), 390 (4.44), 475 (5.00), 708 (3.92), 876 (4.19). ^{1}H NMR (500 MHz, $CDCl_3$): δ 6.62 (2H, d, J = 4.7 Hz, 9,18-H), 7.09 (2H, dd, J = 1.3, 7.7 Hz, 2,4-H), 7.17 (2H, s, 13,14-H), 7.27−7.33 (4H, m), 7.39−7.44 (6H, m), 7.45−7.48 (14H, m). ^{1}H NMR (500 MHz, TFA/$CDCl_3$): δ 5.29 (1H, br s, 22-H), 7.22 (2H, d, J = 4.9 Hz, 9,18-H), 7.36 (2H, dd, J = 1.2, 7.8 Hz, 2,4-H), 7.56 (4H, d, J = 7.6 Hz), 7.61 (4H, d, J = 7.6 Hz), 7.64−7.71 (6H, m), 7.75 (4H, t, J = 7.6 Hz), 7.80 (1H, t, J = 7.8 Hz, 3-H), 7.89 (2H, t, J = 7.4 Hz), 7.97 (2H, d, J = 4.9 Hz, 8,19-H), 7.98 (2H, s, 13,14-H). ^{13}C NMR ($CDCl_3$): δ 113.0, 126.8, 127.9, 128.4, 128.8, 129.0, 129.89, 129.96, 131.3, 132.8, 133.2, 135.7, 137.1, 138.9, 139.9, 143.1, 147.9, 154.8, 155.0, 172.2. ^{13}C NMR (TFA/$CDCl_3$): δ 100.2, 129.0, 129.5, 129.6, 129.8, 131.7, 132.5, 132.6, 135.0, 135.2, 135.9, 137.7, 138.7, 139.8, 140.0, 142.0, 143.3, 154.4, 156.8, 164.1. HRMS (EI) m/z: calcd for $C_{46}H_{30}N_2S$, 642.2129; found, 642.2130.

3-*tert*-Butyl-6,11,16,21-tetraphenyl-24-thiabenziporphyrin (17b). Using the foregoing procedure for **17a**, dicarbinol **16a**[35] (85.8 mg, 0.29 mmol) was reacted with **8b** (128.7 mg, 0.29 mmol) to give thiabenziporphyrin **17b** (61.5 mg, 0.088 mmol, 30%) as a dark solid. Mp: 210−212 °C (dec). UV−vis (1% Et_3N/CH_2Cl_2) λ_{max} (log ε): 342 (4.37), 416 (4.69), 643 (3.98). UV−vis (1% TFA/CH_2Cl_2) λ_{max} (log ε): 344 (4.36), 398 (4.43), 477 (4.99), 703 (3.94), 880 (4.16). ^{1}H NMR (500 MHz, $CDCl_3$): δ 1.00 (9H, s, *t*-Bu), 6.64 (2H, d, J = 4.7 Hz, 9,18-H), 7.04 (1H, t, J = 1.5 Hz, 22-H), 7.10 (2H, d, J = 1.5 Hz, 2,4-H), 7.20 (2H, s, 13,14-H), 7.31 (2H, d, J = 4.7 Hz, 8,19-H), 7.39−7.49 (20H, m, 4 × Ph). ^{1}H NMR (500 MHz, TFA/$CDCl_3$): δ 1.09 (9H, s, *t*-Bu), 4.95 (1H, t, J = 1.5 Hz, 22-H), 7.23 (2H, d, J = 5.0 Hz, 9,18-H), 7.35 (2H, d, J = 1.5, 2,4-H), 7.57 (4H, d, J = 8.0 Hz), 7.62−7.71 (10H, m), 7.77 (4H, t, J = 7.8 Hz), 7.90 (2H, t, J = 7.5 Hz), 7.97 (2H, d, J = 5.0 Hz, 8,19-H), 8.00 (2H, s, 13,14-H). ^{13}C NMR ($CDCl_3$): δ 31.0, 34.7, 110.8, 127.6, 127.9, 128.4, 128.9, 129.6, 129.9, 131.4, 131.5, 133.0, 135.6, 137.2, 139.0, 139.3, 143.4, 148.6, 150.7, 154.69, 154.75, 171.9. ^{13}C NMR (TFA/$CDCl_3$): δ 30.4, 35.5, 98.1, 128.8, 129.2, 129.5, 129.8, 131.6, 132.6, 134.9, 135.4, 135.7, 136.0, 138.4, 139.7, 140.0, 141.9, 143.0, 154.2, 156.6, 157.3, 163.7. HRMS (EI) m/z: calcd for $C_{50}H_{38}N_2S$, 698.2756; found, 698.2750.

6,11,16,21-Tetraphenyl-24-oxabenziporphyrin (17c). Nitrogen was bubbled through a solution of furandicarbinol **16b**[36] (81.3 mg, 0.29 mmol) and benzitripyrrane **8a** (112.5 mg, 0.29 mmol) in dichloromethane (90 mL) for 10 min, and 200 μL of a 10% BF_3·Et_2O solution in dichloromethane was then added. The resulting solution was stirred in the dark at room temperature under nitrogen for 2 h. TFA (2 mL) was added, immediately followed by DDQ (194 mg), and the mixture was stirred for a further 30 min. The solution was washed with water, 5% aqueous sodium bicarbonate solution, water, and 10% hydrochloric acid. The solvent was evaporated under reduced pressure, and the residue was purified by column chromatography on silica, eluting initially with chloroform and then with 1−2% methanol/chloroform. The product fraction was repurified on a second silica column, affording a dark-green band. Evaporation of the solvent under reduced pressure gave the oxabenziporphyrin in a partially protonated form (43.4 mg, 0.081 mmol, 28%) as shiny dark crystals. Mp: >300 °C. UV−vis (5% Et_3N/CH_2Cl_2) λ_{max} (log ε): 385 (4.29), 637 (3.79). UV−vis (CH_2Cl_2) λ_{max} (log ε): 274 (4.62), 377 (4.18), 448 (4.38), 730 (sh, 3.82), 807 (4.13). UV−vis (1% TFA/CH_2Cl_2) λ_{max} (log ε): 380 (4.27), 454 (4.79), 617 (3.71), 758 (3.87). ^{1}H NMR (500 MHz, TFA/$CDCl_3$): δ 5.65 (1H, br t, J = 1.5 Hz, 22-H), 6.98 (2H, dd, J = 1.4, 5.0 Hz, 9,18-H), 7.31 (2H, dd, J = 1.5, 7.8 Hz, 2,4-H), 7.48 (2H, s, 13,14-H), 7.53 (4H, d, J = 7.6 Hz), 7.58 (4H, d, J = 8.0 Hz), 7.62 (4H, t, J = 7.6 Hz), 7.67 (2H, t, J = 7.4 Hz), 7.74 (4H, t, J = 7.8 Hz), 7.81 (2H, dd, J = 1.6, 5.0 Hz, 8,19-H), 7.85−7.88 (3H, m), 11.24 (2H, br s, 2 × NH). ^{13}C NMR (TFA/$CDCl_3$): δ 104.4, 114.5, 129.4, 129.5, 129.7, 131.2, 132.6, 133.2, 134.6, 134.7, 134.8, 135.9, 138.05, 138.08, 138.9, 144.3, 157.5, 163.5. HRMS (ESI) m/z: calcd for $C_{46}H_{30}N_2O$ + H, 627.2436; found, 627.2450.

3-*tert*-Butyl-6,11,16,21-tetraphenyl-24-oxabenziporphyrin (17d). Furandicarbinol **8b** (81.3 mg was reacted with **16b**[36] (128.7 mg, 0.29 mmol) under the foregoing conditions for **17c** to give **17d**·HCl (45.4 mg, 0.080 mmol, 28%) as shiny dark crystals. Mp: >300 °C. UV−vis (5% Et_3N/CH_2Cl_2) λ_{max} (log ε): 395 (4.25), 445 (sh, 4.06), 602 (3.72). UV−vis (CH_2Cl_2) λ_{max} (log ε): 265 (4.55), 352 (4.27), 381 (4.09), 452 (4.37), 730 (sh, 3.75), 806 (4.09). UV−vis (1% TFA/CH_2Cl_2) λ_{max} (log ε): 352 (4.25), 384 (4.12), 456 (4.68), 768 (3.76). ^{1}H NMR (500 MHz, TFA/$CDCl_3$): δ 1.13 (9H, s, *t*-Bu), 5.30 (1H, t, J = 1.5 Hz, 22-H), 7.00 (2H, dd, J = 1.6, 5.1 Hz, 9,18-H), 7.31 (2H, d, J = 1.4 Hz, 2,4-H), 7.50 (2H, s, 13,14-H), 7.54 (4H, d, J = 7.6 Hz), 7.60 (4H, d, J = 8.0 Hz), 7.63 (4H, t, J = 7.7 Hz), 7.68 (2H, t, J = 7.4 Hz), 7.76 (4H, t, J = 7.9 Hz), 7.83 (2H, dd, J = 1.8, 5.1 Hz, 8,19-H), 7.89 (2H, t, J = 7.5 Hz), 11.05 (2H, s, 2 × NH). ^{13}C NMR (TFA/$CDCl_3$): δ 30.5, 35.6, 101.7, 114.5, 129.2, 129.5, 129.7, 131.2, 132.7, 134.72, 134.78, 135.7, 136.1, 137.9, 138.6, 138.9, 144.2, 157.3, 158.1, 161.1, 163.3. HRMS (EI) m/z: calcd for $C_{50}H_{38}N_2O$ + H, 683.3062; found, 683.3071.

Crystallographic Experimental Details for 13b·0.5C_6H_{14}. X-ray-quality crystals of palladium complex **13b**·0.5C_6H_{14} ($C_{45}H_{44}N_3Pd$) were obtained by vapor diffusion of hexane into a chloroform solution of the compound. The crystals were suspended in mineral oil at ambient temperature, and a suitable crystal was selected. The thereby-obtained mineral-oil-coated red needle with approximate dimensions of 0.005 mm × 0.01 mm × 0.12 mm was mounted on a 50 μm MicroMesh MiTeGen micromount and transferred to a Bruker AXS SMART APEX CCD X-ray diffractometer. The X-ray diffraction data were collected at 100(2) K using Mo K_α radiation (λ = 0.71073 Å). A total of 2556 frames were collected. The total exposure time was 127.80 h. The frames were integrated with the Bruker SAINT software package using a narrow-frame algorithm.[37] Integration of the data using a monoclinic unit cell yielded a total of 82 747 reflections to a maximum θ angle of 29.306° (0.73 Å resolution), of which 9535 were independent (average redundancy 8.678, completeness = 99.9%, R_{int} = 10.82%, R_{sig} = 7.08%) and 6719 (70.47%) were observed with $F_o^2 > 2\sigma(F_o^2)$. The final cell constants a = 10.3442(3) Å, b = 29.4631(8) Å, c = 11.8597(3) Å, β = 105.406(2)°, and volume = 3484.63(17) Å^3 are based upon the refinement of the *XYZ* centroids of 9379 reflections above 20$\sigma(I)$ with 4.5° < 2θ < 53.26°. Limiting indices were as follows: $-14 \le h \le 14$, $-40 \le k \le 40$, $-16 \le l \le 16$. Data were corrected for absorption effects using the multiscan method (SADABS).[37] The ratio of minimum to maximum apparent transmission was 0.788 with minimum and maximum SADABS-generated transmission coefficients of 0.588 and 0.746. Solution and data analysis were performed using the WinGX software package.[38] The structure was solved and refined in the space group $P2_1/c$ (No. 14) with Z = 4.[39] The solution was achieved by charge-flipping methods using the program SUPERFLIP,[40,41] and the refinement was completed using the program SHELX2013.[42,43] Residual electron density consistent with disordered hexane was clearly identified, but no suitable model for the hexane was found. The solvent electron density was near

dx.doi.org/10.1021/jo401365p | J. Org. Chem. 2013, 78, 9143−9152

special positions. SQUEEZE was used to "remove" the solvent from the original *hkl* file. SQUEEZE found 58 electrons in each of the voids that contained hexane (50 electrons). Final refinement was carried out using the SQUEEZE-modified *hkl* file. All non-H atoms were refined anisotropically. All H atoms were included in the refinement in the riding-model approximation [C−H = 0.95, 0.98, and 0.99 Å for Ar−H, CH_3, and CH_2; $U_{iso}(H) = 1.2U_{eq}(C)$, except for methyl groups, where $U_{iso}(H) = 1.5U_{eq}(C)$]. Full-matrix least-squares refinement on F^2 led to convergence [$(\Delta/\sigma)_{max} = 0.001$, $(\Delta/\sigma)_{mean} = 0.000$] with $R_1 = 0.0467$ and $wR_2 = 0.0929$ for 6719 data with $F_o^2 > 2\sigma(F_o^2)$ using zero restraints and 420 parameters. A final difference Fourier synthesis showed features in the range of $\Delta\rho_{max} = 0.644$ e$^-$/Å^3 to $\Delta\rho_{min} = -1.173$ e$^-$/Å^3. All residual electron density away from the solvent was within accepted norms and deemed to have no chemical significance. Molecular diagrams were generated using ORTEP-3.[38] CCDC 952780 contains the supplementary crystallographic data for this paper. These data can be obtained free of charge from the Cambridge Crystallographic Data Centre via www.ccdc.cam.ac.uk/data_request/cif.

■ ASSOCIATED CONTENT

Supporting Information

Selected ^{1}H NMR, ^{1}H−^{1}H COSY, HSQC, ^{13}C NMR, MS, and UV−vis spectra and a CIF for the X-ray structure of **13b**. This material is available free of charge via the Internet at http://pubs.acs.org.

■ AUTHOR INFORMATION

Corresponding Author

*E-mail: tdlash@ilstu.edu.

Notes

The authors declare no competing financial interest.

■ ACKNOWLEDGMENTS

This work was supported by the National Science Foundation under Grants CHE-0911699 and CHE-1212691 and by the Petroleum Research Fund, administered by the American Chemical Society. The authors also thank NSF (Grant CHE-1039689) for providing funding for the X-ray diffractometer.

■ REFERENCES

(1) Lash, T. D.; Chaney, S. T.; Richter, D. T. *J. Org. Chem.* **1998**, *63*, 9076−9088.
(2) Stępień, M.; Latos-Grażyński, L. *Acc. Chem. Res.* **2005**, *38*, 88−98.
(3) Berlin, K.; Breitmaier, E. *Angew. Chem., Int. Ed. Engl.* **1994**, *33*, 1246−1247.
(4) Lash, T. D. *Angew. Chem., Int. Ed. Engl.* **1995**, *34*, 2533−2535.
(5) Stępień, M.; Latos-Grażyński, L. *Chem.—Eur. J.* **2001**, *7*, 5113−5117.
(6) Richter, D. T.; Lash, T. D. *Tetrahedron* **2001**, *57*, 3659−3673.
(7) Lash, T. D.; Szymanski, J. T.; Ferrence, G. M. *J. Org. Chem.* **2007**, *72*, 6481−6492.
(8) Lash, T. D.; Yant, V. R. *Tetrahedron* **2009**, *65*, 9527−9535.
(9) (a) Huang, C.; Li, Y.; Yang, J.; Cheng, N.; Liu, H.; Li, Y. *Chem. Commun.* **2010**, *46*, 3161−3163. (b) Chang, G.-F.; Kumar, A.; Ching, W.-M.; Chu, H.-W.; Hung, C.-H. *Chem.—Asian J.* **2009**, *4*, 164−173.
(10) Lash, T. D.; Miyake, K.; Xu, L.; Ferrence, G. M. *J. Org. Chem.* **2011**, *76*, 6295−6308.
(11) (a) Stępień, M.; Latos-Grażyński, L.; Szterenberg, L.; Panek, J.; Latajka, Z. *J. Am. Chem. Soc.* **2004**, *126*, 4566−4580. (b) Stępień, M.; Latos-Grażyński, L.; Szterenberg, L. *Inorg. Chem.* **2004**, *43*, 6654−6662. (c) Hung, C.-H.; Chang, F.-C.; Lin, C.-Y.; Rachlewicz, K.; Stępień, M.; Latos-Grażyński, L.; Lee, G.-H.; Peng, S.-M. *Inorg. Chem.* **2004**, *43*, 4118−4120.
(12) Lash, T. D.; Rasmussen, J. M.; Bergman, K. M.; Colby, D. A. *Org. Lett.* **2004**, *6*, 549−552.
(13) Hung, C.-H.; Chang, G.-F.; Kumar, A.; Lin, G.-F.; Luo, L.-Y.; Ching, W.-M.; Diau, E. W.-G. *Chem. Commun.* **2008**, 978−980.
(14) Lash, T. D.; Young, A. M.; Rasmussen, J. M.; Ferrence, G. M. *J. Org. Chem.* **2011**, *76*, 5636−5651.
(15) Ziegler, C. J. In *Handbook of Porphyrin Science—With Applications to Chemistry, Physics, Materials Science, Engineering, Biology and Medicine*; Kadish, K. M., Smith, K. M., Guilard, R., Eds.; World Scientific Publishing: Singapore, 2012; Vol. *17*, pp 114−238.
(16) Vogel, E. *J. Heterocycl. Chem.* **1996**, *33*, 1461−1487.
(17) Lash, T. D. *J. Porphyrins Phthalocyanines* **2011**, *15*, 1093−1115.
(18) (a) Nakagami, Y.; Sekine, R.; Aihara, J.-i. *Org. Biomol. Chem.* **2012**, *10*, 5219−5229. (b) Aihara, J.-i.; Nakagami, Y.; Sekine, R.; Makino, M. *J. Phys. Chem. A* **2012**, *116*, 11718−11730.
(19) Wu, J. I.; Fernandez, I.; Schleyer, P. v. R. *J. Am. Chem. Soc.* **2013**, *135*, 315−321.
(20) Lash, T. D. In *Handbook of Porphyrin Science—With Applications to Chemistry, Physics, Materials Science, Engineering, Biology and Medicine*; Kadish, K. M., Smith, K. M., Guilard, R., Eds.; World Scientific Publishing: Singapore, 2012; Vol. *16*, pp 1−329.
(21) For examples of hetero-oxybenziporphyrins and heterocarbaporphyrins, see: (a) Liu, D.; Lash, T. D. *Chem. Commun.* **2002**, 2426−2427. (b) Venkatraman, S.; Anand, V. G.; Pushpan, S. K.; Sankar, J.; Chandrashekar, T. K. *Chem. Commun.* **2002**, 462−463. (c) Liu, D.; Ferrence, G. M.; Lash, T. D. *J. Org. Chem.* **2004**, *69*, 6079−6093. (d) Lash, T. D.; Lammer, A. D.; Ferrence, G. M. *Angew. Chem., Int. Ed.* **2012**, *51*, 10871−10875.
(22) For an example of an N-confused thiapyriporphyrin, see: Mysliborski, R.; Rachlewicz, K.; Latos-Grażyński, L.; Szterenberg, L. *Inorg. Chem.* **2006**, *45*, 7828−7834.
(23) For an example of a thia-*p*-benziporphyrin, see: Hung, C.-H.; Lin, C.-Y.; Lin, P.-Y.; Chen, Y.-J. *Tetrahedron Lett.* **2004**, *45*, 129−132.
(24) For examples of hetero-N-confused porphyrins, see: (a) Heo, P.-Y.; Lee, C.-H. *Tetrahedron Lett.* **1996**, *37*, 197−200. (b) Heo, P.-Y.; Lee, C.-H. *Bull. Korean Chem. Soc.* **1996**, *17*, 515−520. (c) Lee, C.-H.; Kim, H.-J. *Tetrahedron Lett.* **1997**, *38*, 3935−3938. (d) Lee, C.-H.; Kim, H.-J.; Yoon, D.-W. *Bull. Korean Chem. Soc.* **1999**, *20*, 276−280. (e) Yoon, C.-H.; Lee, C.-H. *Bull. Korean Chem. Soc.* **2000**, *21*, 618−622. (f) Pushpan, S. K.; Srinivasan, A.; Anand, V. R. G.; Chandrashekar, T. K.; Subramaniam, A.; Roy, R.; Siguira, K.-i.; Sakata, Y. *J. Org. Chem.* **2001**, *66*, 153−161. (g) Pacholska, E.; Latos-Grażyński, L.; Szterenberg, L.; Ciunik, Z. *J. Org. Chem.* **2000**, *65*, 8188−8196. (h) Sprutta, N.; Latos-Grażyński, L. *Org. Lett.* **2001**, *3*, 1933−1936.
(25) For examples of heteroazuliporphyrins, see: (a) Graham, S. R.; Colby, D. A.; Lash, T. D. *Angew. Chem., Int. Ed.* **2002**, *41*, 1371−1374. (b) Venkatraman, S.; Anand, V. G.; PrabhuRaja, V.; Rath, H.; Sankar, J.; Chandashekar, T. K.; Teng, W.; Senge, K. R. *Chem. Commun.* **2002**, 1660−1661. (c) Lash, T. D.; Colby, D. A.; Graham, S. R.; Chaney, S. T. *J. Org. Chem.* **2004**, *69*, 8851−8864.
(26) Results presented in part at the 245th ACS National Meeting. See: Toney, A. M.; Lash, T. D. *Abstr. Pap.—Am. Chem. Soc.* **2013**, *245*, CHED-1113.
(27) Lash, T. D.; Pokharel, K.; Serling, J. M.; Yant, V. R.; Ferrence, G. M. *Org. Lett.* **2007**, *9*, 2863−2866.
(28) Stępień, M.; Szyszko, B.; Latos-Grażyński, L. *Org. Lett.* **2009**, *11*, 3930−3933.
(29) Maeda, H.; Osuka, A.; Ishikawa, Y.; Aritome, I.; Hisaeda, Y.; Furuta, H. *Org. Lett.* **2003**, *5*, 1293−1296.
(30) Furuta, H.; Kubo, N.; Maeda, H.; Ishizuka, T.; Osuka, A.; Nanami, H.; Ogawa, T. *Inorg. Chem.* **2000**, *39*, 5424−5425.
(31) Ishizuka, T.; Yamasaki, H.; Osuka, A.; Furuta, H. *Tetrahedron* **2007**, *63*, 5137−5147.
(32) Lash, T. D.; Young, A. M.; Von Ruden, A. L.; Ferrence, G. M. *Chem. Commun.* **2008**, 6309−6311.
(33) Allen, F. H. *Acta Crystallogr.* **2002**, *B58*, 380−388.
(34) Tardieux, C.; Bolze, F.; Gros, C. P.; Guilard, R. *Synthesis* **1998**, 267−268.
(35) (a) Stilts, C. E.; Nelen, M. I.; Hilmey, D. G.; Davies, S. R.; Gollnick, S. O.; Oseroff, A. R.; Gibson, S. L.; Hilf, R.; Detty, M. R. *J.*

Med. Chem. **2000**, *43*, 2403−2410. (b) Hilmey, D. G.; Abe, M.; Nelen, M. I.; Stilts, C. E.; Baker, G. A.; Baker, S. N.; Bright, F. V.; Davies, S. R.; Gollnick, S. O.; Oseroff, A. R.; Gibson, S. L.; Hilf, R.; Detty, M. R. *J. Med. Chem.* **2002**, *45*, 449−461.
(36) Chmielewski, P. J.; Latos-Grażyński, L.; Olmstead, M. M.; Balch, A. L. *Chem.—Eur. J.* **1997**, *3*, 268−278.
(37) *APEX2*, version 2013.2-0; Bruker AXS Inc.: Madison, WI, 2013.
(38) Farrugia, L. J. *J. Appl. Crystallogr.* **2012**, *45*, 849−854.
(39) McArdle, P. *J. Appl. Crystallogr.* **1996**, *29*, 306.
(40) Palatinus, L.; Chapuis, G. *J. Appl. Crystallogr.* **2007**, *40*, 786−790.
(41) Palatinus, L.; Prathapa, S. J.; van Smaalen, S. *J. Appl. Crystallogr.* **2012**, *45*, 575−580.
(42) Sheldrick, G. M. *Acta Crystallogr.* **2008**, *A64*, 112−122.
(43) Sheldrick, G. M. *SHELX2013*; University of Göttingen: Göttingen, Germany, 2013.